

## Effect of duration of synaptic activity on spike rate of a Hodgkin-Huxley neuron with delayed feedback

M. Hashemi, A. Valizadeh, and Y. Azizi

*Institute for Advanced Studies in Basic Sciences, P.O. Box 45195-1159, Zanjan, Iran*

(Received 14 November 2010; revised manuscript received 28 October 2011; published 21 February 2012)

A recurrent loop consisting of a single Hodgkin-Huxley neuron influenced by a chemical excitatory delayed synaptic feedback is considered. We show that the behavior of the system depends on the duration of the activity of the synapse, which is determined by the activation and deactivation time constants of the synapse. For the fast synapses, those for which the effect of the synaptic activity is small compared to the period of firing, depending on the delay time, spiking with single and multiple interspike intervals is possible and the average firing rate can be smaller or larger than that of the open loop neuron. For slow synapses for which the synaptic time constants are of order of the period of the firing, the self-excitation increases the firing rate for all values of the delay time. We also show that for a chain consisting of few similar oscillators, if the synapses are chosen from different time constants, the system will follow the dynamics imposed by the fastest element, which is the oscillator that receives excitations via a slow synapse. The generalization of the results to other types of relaxation oscillators is discussed and the results are compared to those of the loops with inhibitory synapses as well as with gap junctions.

DOI: [10.1103/PhysRevE.85.021917](https://doi.org/10.1103/PhysRevE.85.021917)

PACS number(s): 87.19.lr, 87.19.lg, 87.19.lm

### I. INTRODUCTION

A very crucial step in the study of complex collective phenomena in large networks is to investigate the behavior of the few component circuits known as the *network motifs*, since some of these microcircuits are known to be the building blocks of the large networks [1]. Among the most prevalent motifs as the basic microcircuits constructing recurrent networks are loops and chains [2,3]. Recurrent networks are known as base structures for creating short- and long-term memory [4]. An elementary preparation for the study of chains is a one element loop with fixed delayed feedback stimulation. This simple model can explain the behavior of a neuron with *autaptic* self-connection [5] and also is useful for understanding the more complex loops consisting of several elements which are more frequent in the neural systems [6].

Delayed self-communication is of particular interest as its regulatory role in nature and technology [7]. Excitable gene regulatory systems [8], eye movements [9], human balance [10], and optically communicating semiconductor lasers [11,12] are a few examples. In neural communication, due to the finite speed of the data transfer in the axons and dendrites, and possible processing latency in the synapses, communicating between the different areas may take delays from few to hundreds of milliseconds, so significant, compared to the time scales of the neuronal activities [13,14].

A delayed feedback has a nontrivial impact on the dynamics of the nonlinear oscillators. With delayed feedback, more complex dynamics are likely to occur due to the infinite dimension of the dynamical system [15]. Multistability and chaos are two widely reported effects of the delayed feedback both in theoretical studies [16,17] and in experiments on neurons [18] and on laser oscillators [19]. On the other hand, self-stimulation with fixed delay time can suppress chaos and induce order in the dynamics of the nonlinear oscillators [20]. For ensembles of oscillators, a mean-field delayed feedback is proposed to control synchronization, i.e., it can either result

in increase or destroy the coherence of the systems of coupled oscillators [21,22].

Multistability induced by the delayed feedback poses the loops as the systems with memory [16]. In neural systems, delayed feedback has been proposed to be responsible for precise firing of basket cells in hippocampus during Theta and Gamma rhythms. Experiments show that delayed recurrent excitations are capable of regulating the structure of the interspike intervals in the presence of noise [5]. An early experimental study of the pacemaker cells of crayfish [23] followed by numerical studies led to the deduction that delayed self-coupling besides neuronal adaptation can result in bursting, high frequency discharges interrupted by relatively long quiescent intervals [24]. It was argued that the effect of self-excitation has been to increase the firing rate during the bursts where a reduction of excitability during high activity drives the neuron in the quiescent interval [24]. Later it was shown that for small strength of self-coupling both acceleration and deceleration of neuronal activity are possible. It has been argued that existence of unstable fixed points in the phase space of the system are responsible for the slowing down of an oscillator activity with self-coupling [25].

In this paper we first study the dynamics of single neuron when it is influenced by a delayed self-coupling and then will show how the results can be generalized to neuronal loops with more than one neuron. Both one and two neuron loops appear as the basic blocks for canonical arrangements proposed as a possible explanation for the distant isochronous synchronization in the brain [2,26]. A similar arrangement with a thermally sensitive neuron has been studied with the emphasis on the effect of feedback on the frequency and amplitude of sustained subthreshold oscillations [27]. Also both the single element loop with an optical delayed feedback or the chains of semiconductor lasers as the nonlinear oscillators has been widely studied [11,12].

We have considered the Hodgkin-Huxley (HH) model as a generic model for excitable and oscillating membranes but

the results have been argued to be qualitatively general for all the relaxation oscillators, e.g., FitzHugh-Nagumo oscillators, while they inherit the type of excitability of the HH model. A quantitative characterization of the response of the model can be achieved by considering phase-reset curves (PRCs), which are related to the type of excitability of the oscillator [28]. The curves determine how inputs to an oscillator shift its timing or phase and are characterized by the type of the bifurcation, which changes the system from excitable to oscillatory [29]. Infinite period (saddle node on invariant circle) bifurcation leads to type-I PRCs, which are mainly positive while type-II PRCs with a large negative region are characterized by Hopf bifurcation [29]. The Hodgkin-Huxley model with the classical parameters is known as a type-II excitable system and we see that the response of the feedback system is retained while a type-II oscillator is considered.

Most of the previous studies on the effect of the self-stimulation on the neurons have been done with a linear self-coupling, which determines a gap junction [16,27]. Here, by considering a chemical self-coupling, we aim to study the effect of the duration of the activity of the synapse on the behavior of the model. For excitatory chemical synapses, AMPA receptors show a fast action to the release of glutamate, activating in tens of microseconds and deactivating in a few milliseconds. Instead, the activating time of NMDA receptors is of order of milliseconds where deactivating times range from tens to hundreds of milliseconds [30]. This wide range of activity time of synapses brings up the question of how the effect of feedback may be dependent on the time constants of the synapse, i.e., the duration of the synaptic activity. While the main body of our study focuses on how the average rate of firing is influenced by the synaptic feedback with different time constants of activation and deactivation, the dependence of the interspike intervals (ISIs) to these parameters is also investigated.

The HH model with an external current input shows two successive bifurcations: a saddle-node bifurcation of limit cycles and an inverse Hopf bifurcation [31]. In this study, the open loop neuron has been assumed to be in a bistable state between two bifurcations where both a limit cycle and a stable fixed point are present in the phase space of the model. We have also considered the case in which the open loop neuron is excitable near the first bifurcation point and also comment about what is expectable if the only attractor of the system is the limit cycle. Some of the results are compared with the loops with inhibitory synapses and also with gap junctions.

The paper is organized as follows: in subsequent section we describe the model equations and parameters, Sec. III governs the main results for a single element loop, and in Sec. IV the results have been presented for the chains with more than one neuron. In Sec. V using the characteristic diagram of the neuron, we show how the firing rate of the neuron may be entrained by the feedback loop. Section VI is devoted to the conclusion and in the Appendix, phase reset curves of the models used in the paper are given.

## II. MODEL

The HH model serves as a paradigm for real spiking neurons based on the dynamic conductance of ion currents [32]. We

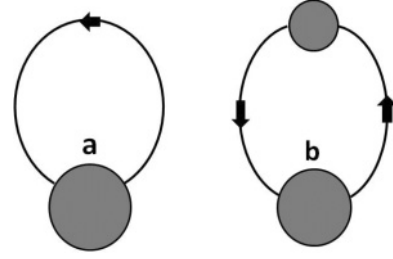


FIG. 1. A recurrent loop consisting of a single neuron (a) and two neurons (b).

consider a HH neuron with a self-stimulation (see Fig. 1) whose membrane voltage is described by

$$c \frac{dv}{dt} + I_{Na} + I_K + I_l + I_{syn} = I_{ext}. \quad (2.1)$$

$c$  is the capacitance per unit area of the membrane, which is taken as  $1 \mu F/cm^2$  and  $I_{ext}$  stands for the external current.  $I_l = g_l(v - E_l)$  is the passive leak current and  $I_{Na} = \bar{g}_{Na} m^3 h (v - E_{Na})$  and  $I_K = \bar{g}_K n^4 (v - E_K)$  are sodium and potassium currents, respectively.  $g_l = 0.3 \text{ mS/cm}^2$  is the conductance for the leak current and  $\bar{g}_{Na} = 120 \text{ mS/cm}^2$  and  $\bar{g}_K = 36 \text{ mS/cm}^2$  are the maximum conductance for the sodium and potassium ions, and  $E_l = 10.6 \text{ mV}$ ,  $E_{Na} = 115 \text{ mV}$ , and  $E_K = -12 \text{ mV}$  are reversal voltages for the leak, sodium, and potassium currents, respectively.  $m$  ( $h$ ), activation (inactivation) variable of sodium, and  $n$ , activation variable of potassium, obey the differential equations

$$\begin{aligned} \frac{dm}{dt} &= \alpha_m(1 - m) - \beta_m m, \\ \frac{dh}{dt} &= \alpha_h(1 - h) - \beta_h h, \\ \frac{dn}{dt} &= \alpha_n(1 - n) - \beta_n n, \end{aligned} \quad (2.2)$$

where  $\alpha$  and  $\beta$  are functions of membrane voltage as can be found in [32].

To model the electrical synapses, a linear coupling is used after modulating by a threshold function  $f(v - v_{th})$ ,

$$I_{syn} = -g_{el} v(t - \tau) f(v - v_{th}), \quad (2.3)$$

in which a hard threshold function  $f(x) = 1/2[1 + \tanh(\eta x)]$  is taken with  $\eta = 10$ , and the threshold voltage  $v_{th} = 20 \text{ mV}$  ensures that subthreshold oscillations are not delivered to the gap junction [33].  $g_{el}$  is the synaptic conductivity and  $\tau$  is the loop delay time.

With a chemical synapse the feedback synaptic current is described by  $I_{syn} = \bar{g}_{syn} s(t - \tau)(v - E_{syn})$  where  $\bar{g}_{syn}$  is the synaptic maximum conductivity,  $E_{syn}$  is the synaptic reversal potential, and  $\tau$  is the delay of the feedback loop.  $s(t)$  is the synaptic activity function defined via

$$\frac{ds}{dt} = \alpha f(v - v_{th})(1 - s) - \beta s, \quad (2.4)$$

with  $\alpha$  and  $\beta$  defining the activation and deactivation time constants,  $v_{th} = 20 \text{ mV}$  is the threshold voltage for the activation of the synapse, and  $f$  is the threshold function as defined in the text following Eq. (2.3) [33].

The parameters we have chosen are such that with  $I_{\text{ext}} = 0$ , the resting potential of the neuron is zero; so we have taken  $E_{\text{syn}} = 80$  mV for excitatory neurons and  $E_{\text{syn}} = 0$  for inhibitory neurons. Inspired by typical time constants of the activation and deactivation of excitatory synapses with AMPA and NMDA receptors, we have chosen  $\alpha = 10$  and  $\beta = 0.5$  as the activation and deactivation time constants for fast synapses, and  $\alpha = 1$  and  $\beta = 0.05$  for modeling slow synapses [30].

We also use the FitzHugh-Nagumo (FN) model [34] as a prototype for relaxation oscillators. To model a type-II excitable system we use

$$\begin{aligned} \frac{dv}{dt} &= v - v^3/3 - w - I_{\text{syn}} + I_{\text{ext}}, \\ \frac{dw}{dt} &= 0.08(v + 0.7 - 0.8w), \end{aligned} \quad (2.5)$$

with the  $v$  and  $w$  as the fast (voltage) and slow (recovery) variables, respectively. The synaptic current is again described by Eq. (2.4) but since the spikes in the FN model have different amplitudes, the synaptic voltages for the excitatory and inhibitory neurons are  $E_{\text{syn}} = 1.2$  and  $E_{\text{syn}} = -1.2$ , respectively.

Also a variation of the FN model,

$$\begin{aligned} \frac{dv}{dt} &= v - v^3/3 - w - I_{\text{syn}} + I_{\text{ext}}, \\ \frac{dw}{dt} &= 0.08[2.5 + 2.5 \tanh(\eta v) - w], \end{aligned} \quad (2.6)$$

is used to describe a system with type-I excitability.  $v$  and  $w$  and the synaptic current have the same interpretation as in Eq. (2.5). The model without feedback shows an infinite period bifurcation in  $I_{\text{ext}} = 2/3$  when  $\eta \gg 1$  [35].

Phase reset curves of the three models introduced above are given in the Appendix. In what follows, when it is not explicitly noted, the voltage, current, and conductivity are measured in mV,  $\mu\text{A}/\text{cm}^2$ , and  $\text{mS}/\text{cm}^2$ , respectively, with time in ms and firing rates in  $\text{ms}^{-1}$ .

### III. EFFECT OF THE DELAYED FEEDBACK LOOP ON THE FIRING RATE

In Fig. 2(a), we have shown the average firing rate of the HH neuron vs the delay time  $\tau$  for fast and slow excitatory synapses for the case where the neuron is biased over the threshold such that a limit cycle coexists with a stable fixed point [31]. It can be seen for the slow synapses that the feedback loop always increases the firing rate of the neuron whereas for a fast synapse, the effect of the self-synapse is dependent on the delay time. When the loop synaptic pulse arrives in the neuron around the odd multiples of the half period of firing of the open loop neuron (*intrinsic period*), i.e.,  $\tau \sim (2j + 1)T/2$  with  $T$  being the period of firing of the open loop neuron, the excitatory feedback loop with fast synapse decreases the firing rate and may even suppress the firing. It is also clear that adding multiples of the intrinsic period of the neuron to the delay does not result in the similar behavior. For the fast synapses, the effect of the larger delays is weaker than the delays below the intrinsic period, i.e., the variation of the firing rate with respect to open loop firing is smaller for larger delays. For slow synapses, dependence of the firing rate on

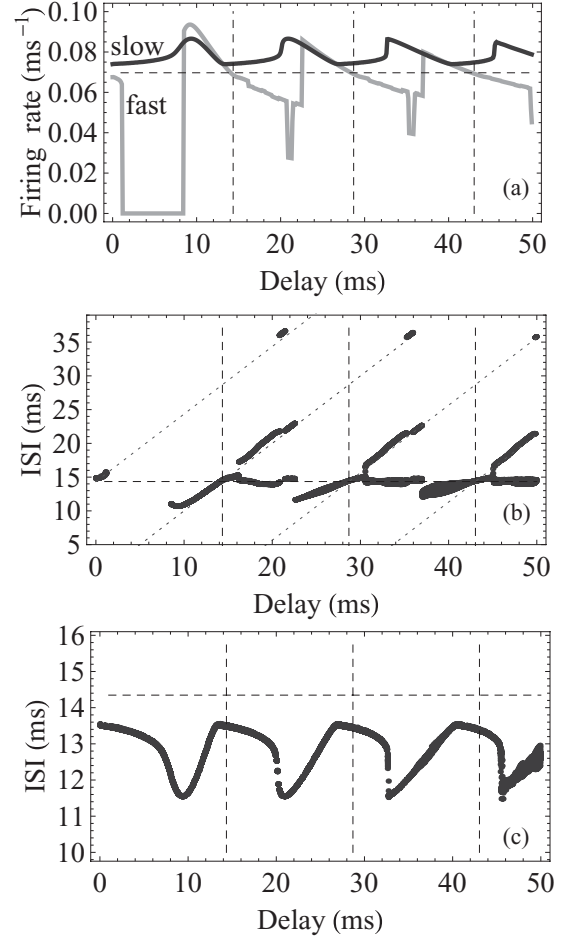


FIG. 2. (a) Mean firing rate of the HH neuron vs loop delay time with an excitatory feedback for the fast (gray) and slow (black) synapses.  $g_{\text{syn}} = 0.05$ ,  $\beta = 0.5$ , and  $\alpha = 10$  for fast and  $\beta = 0.05$  and  $\alpha = 1$  for slow synapses. The horizontal and vertical dashed lines show the intrinsic rate of firing (without feedback) and the multiples of intrinsic period of firing, respectively. The external current  $I_{\text{ext}} = 7\mu\text{A}/\text{cm}^2$  is imposed on the neuron as a step current is switched on at  $t = 0$ . (b) and (c) show the interspike intervals (bifurcation diagram) with fast and slow synapses respectively. The extra inclined dotted lines in (b) are guides to the eye showing when there are ISIs determined by the loop delay time. The equations have been integrated for 2s and the first 200 ms are discarded to ensure that transient effects do not disturb the results. The intervals between successive spikes are recorded in the bifurcation diagram and the total number of spikes divided by the integration time is the mean firing rate.

the delay time is nearly periodic but the period is less than the intrinsic period of the neuron. This is evident as the leftward shift of the maximum of the firing rate for slow synapses, with respect to the vertical dashed lines, which indicates multiples of the intrinsic period.

In Figs. 2(b) and 2(c), we have plotted interspike intervals (ISIs) vs delay time, a *bifurcation diagram* [37] for the fast and slow synapses, respectively. With slow synapses, the model shows a single ISI for all the values of the loop delay time. With fast synapses for the delay time larger than  $T$ , three behaviors are recognizable: for delay time near and greater than multiples of the intrinsic period, the ISIs are not considerably different from intrinsic period, i.e., the feedback loop has a

minor effect on the neuron since all the feedback pulses arrive in the neuron in the refractory period. For delay time near and less than multiples of the open loop period, the effect of the feedback pulses is a notable decrease of the period of the firing. The interesting behavior is observed when the delay time is about odd multiples of the half period of firing of the open loop neuron  $\tau \sim (2j + 1)T/2$ . In this case the ISI can take each of the two time constants present in the system: the intrinsic period of the firing of the open loop neuron and the loop delay time. The synaptic activity here consists of groups with two or more pulses, where just one of them leads to an action potential. A simple explanation for this observation is that for each couple of pulses kicking the neuron via feedback loop, one of them arrives in the refractory period and has no effect on the system. Note that this behavior can be seen when the delay time is more than the intrinsic period of the neuron not considered in [25]. It is also notable that each transition between the states with single ISI and multiple ISIs coincides with an abrupt change of firing rate in Fig. 2(a).

We also explain how the feedback pulses from fast synapses can stop the firing when the delay time is smaller than the intrinsic period, while for large feedback times the firing is not stopped (Fig. 2). In Fig. 3 we have shown the time evolution of the membrane voltage for the system with fast synapse, for three values of delay which differ in one intrinsic period time. A planar representation of the reduced phase space is also given retaining the voltage  $v$  and recovery variable  $n$ . As mentioned before, for the value of the current input we used, the HH neuron shows bistability as a result of coexistence of a stable limit cycle with a stable fixed point. In Fig. 3(a) the pulse suppresses the spiking by sending the phase point to the domain of attraction of the stable focus. This domain is determined by the unstable limit cycle, which is born with the stable limit cycle in a saddle-node bifurcation of limit cycles [31]. For the delay larger than the intrinsic period, before the delayed feedback pulse arrives in neuron, the neuron fires an extra action potential. Hence the action potentials and delayed feedback stimulations are of the form of doublets, with ISI equal to intrinsic period, separated by loop delay time [Fig. 3(b)]. When the first pulse of the doublet sends the system to the basin of attraction of the focus, the second can shoot the system orbit out of the basin and lead to an action potential as can be seen in Fig. 3(b). Yet, small amplitude oscillations around the focus lag the next spike and reduce the rate of the firing. This scenario is also repeated by the triplets when the delay time is larger than twice the intrinsic period [Fig. 3(c)].

For an electrical synapse, since both activation and deactivation are instantaneous, we expect the results to be more similar to those of the fast chemical synapse. As we see in Fig. 4(a), dependence of the firing rate on the loop feedback delay has similar features as the fast chemical synapse but the bifurcation diagram shown in Fig. 4(b) shows different behavior compared to Fig. 2(b), e.g., with electrical synapse aperiodic states are seen for loop delays larger than the intrinsic period. Although for the parameters we have chosen, the two diagrams are different, our arguments above do not rule out the possibility of the similar behavior for a system with electrical synapses. So whether such differences are generic or they can be removed by a suitable choice of parameters is yet an open question.

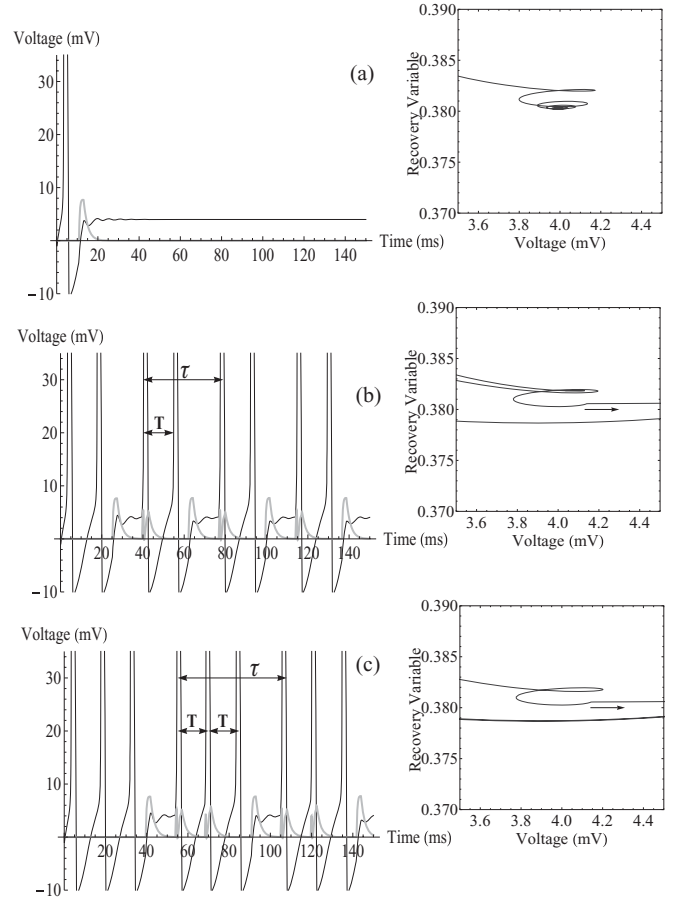


FIG. 3. In (a)–(c) (left panels) the evolution of the membrane voltage of the neuron (black) and the synaptic activity (gray) is plotted for three values of delay  $\tau = 7.5$  ms,  $\tau = T + 7.5$  ms, and  $\tau = 2T + 7.5$  ms, respectively, where  $T \simeq 14.3$  ms is the intrinsic period of the neuron. The synaptic activity function is exaggerated to be distinguishable and the interspike intervals for the doublets in (b) and triplets in (c) are shown by left-right arrows. In the right hand side, against each plot for (a)–(c), a reduced phase space representation around fixed points of the system is given. The arrows in (b) and (c) indicate the effect of the second excitatory pulse in the doublets and triplets.

We have also checked the system with an inhibitory synapse. As it is seen in Fig. 5, in this case the results for both fast and slow chemical synapses are qualitatively similar, i.e., there is no increase of firing rate even when an inhibitory fast synapse is assumed. Suppression of firing is what is naturally expected to occur with inhibitory synapses; here we note that inhibitory inputs via slow synapses may stop firing for a wider range of loop delay time. The bifurcation diagram for such a system [Fig. 5(b)] shows that the inhibitory feedback loop with fast synapses does not lead to multiple ISIs as it had been seen for fast excitatory synapses. This result is worth noting, since it seems the loop delay time cannot be revealed in the dynamics of the system, as we will see also in Sec. V.

Since the effect of the synaptic feedback on the firing rate is dependent on the behavior of the system near the limit cycle and equivalently on the type of the excitability, it is expected for simplified models which inherit the main properties of the HH phase space to show similar behavior as the HH model

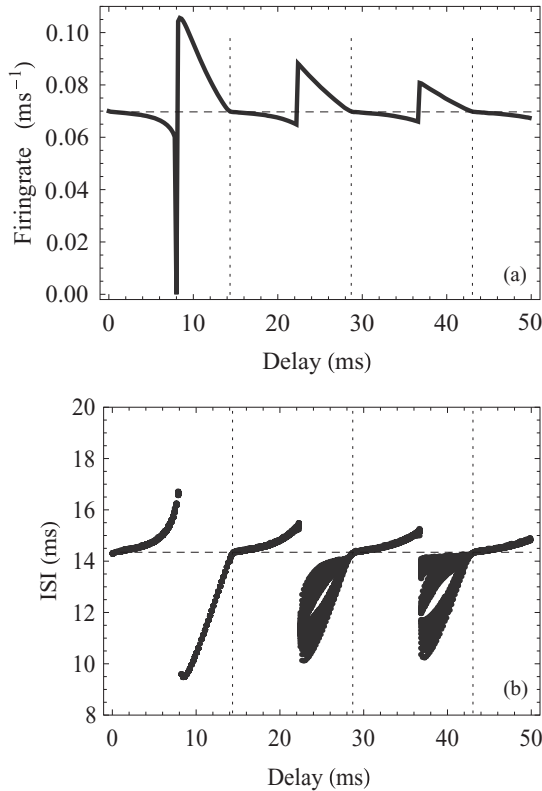


FIG. 4. (a) Mean firing rate and (b) interspike intervals of the HH neuron vs loop delay time with a feedback via an electric synapse.  $g_{el} = 0.05$  and the external current  $I_{ext} = 7 \mu\text{A}/\text{cm}^2$  is imposed on the neuron as a step current switched on at  $t = 0$ . The horizontal dashed lines show the intrinsic rate of firing (without feedback) in (a) and intrinsic period of firing in (b) and the vertical dashed lines show the multiples of intrinsic period of firing.

for such study. A simple type-II model, which saves such properties of the HH equations, is the FN model introduced by Eq. (2.5) (see the Appendix). We repeated the study of the ISIs, with type-II FN neurons: as seen in Fig. 6(a), the behavior of the system under influence of the fast and slow synapses is similar to those of the HH model, which supports the arguments about the origin of the phenomenon. The main difference is that firing death is not seen since, unlike the HH system, here the open loop system is monostable with the limit cycle as the only attractor. Such a behavior can also be seen for the HH model if it is biased with a current by which the system is not bistable and the stable fixed point has lost the stability via inverse (subthreshold) Hopf bifurcation. There are also regions of aperiodic firing for fast synapses where the interspike intervals can take each value of a continuous subset of all possible values both for type-I and type-II FN oscillators [37].

We note in passing that for a type-I oscillator a decrease in the firing rate does not occur for an excitatory fast synaptic feedback. In Fig. 6(b) we have shown the bifurcation diagram for a type-I system (Appendix) introduced by Eq. (2.6). While the two systems in Fig. 6 show a similar response to the self-excitation via slow synapses, fast synaptic feedback always reduces the ISIs leading to larger firing rates for all the delay times. Another notable difference is that the change in the

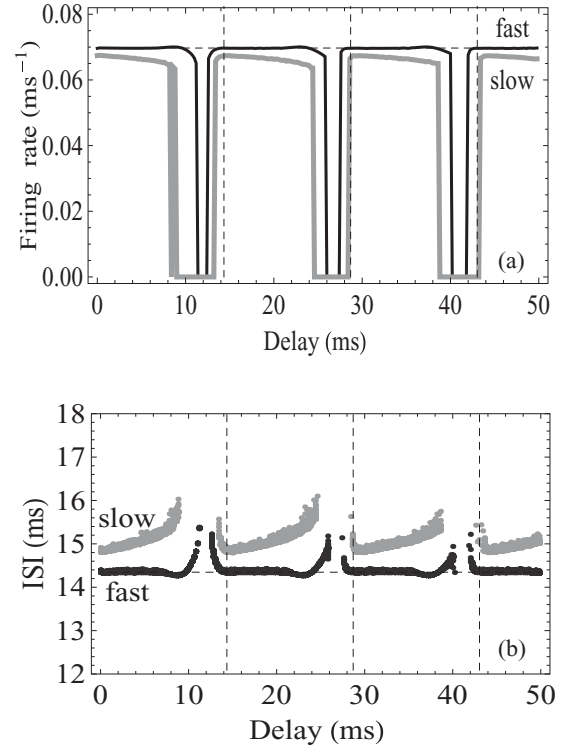


FIG. 5. (a) Mean firing rate and (b) interspike intervals of the HH neuron vs loop delay time with a feedback via a fast (black) and slow (gray) inhibitory synapse.  $g_{syn} = 0.05$ , and  $E_{syn} = 0$  to model an inhibitory synapse and other parameters are the same as Fig. 2. The horizontal dashed lines show the intrinsic rate of firing (without feedback) in (a) and intrinsic period of firing in (b) and the vertical dashed lines show the multiples of intrinsic period of firing.

intervals due to the fast synapses can exceed that of the slow synapse for type-II oscillators. This is reasonable since a kind of integration of the responses around the limit cycle is done by the slow synapse and the response of the system for type-II oscillators is negative in the regions of the limit cycle.

We end this section with a study of the behavior of the system under the influence of the feedback when the open-loop neuron is excitable, i.e., when it is biased slightly below the threshold for repetitive spiking. The results are shown in Fig. 7 with the input current chosen as it causes a single spike at  $t = 0$ . It is shown that the behavior of the system for both fast and slow synapses strongly depends on the delay. It is expected that the neuron remains inactive for small values of delay since the feedback pulse arrives in the refractory period. The threshold delay time for repetitive spiking decreases with increasing the strength of the synapse. For larger value of delay there are again regions with zero activity, arising from the existence of subthreshold oscillation for the HH neuron. For the neurons with sustained sub-threshold oscillations, it is known that exact timing of the arrival of the feedback determines the behavior of the neuron [27,38]. Here we see for damped subthreshold oscillations that again the feedback timing is detected by the neuron activity. The sensitivity of neuron in the after spike oscillating period varies with the period of such oscillations for both fast and slow synapses. If the neuron is in the minimum of such oscillations, larger stimulation is needed to create an

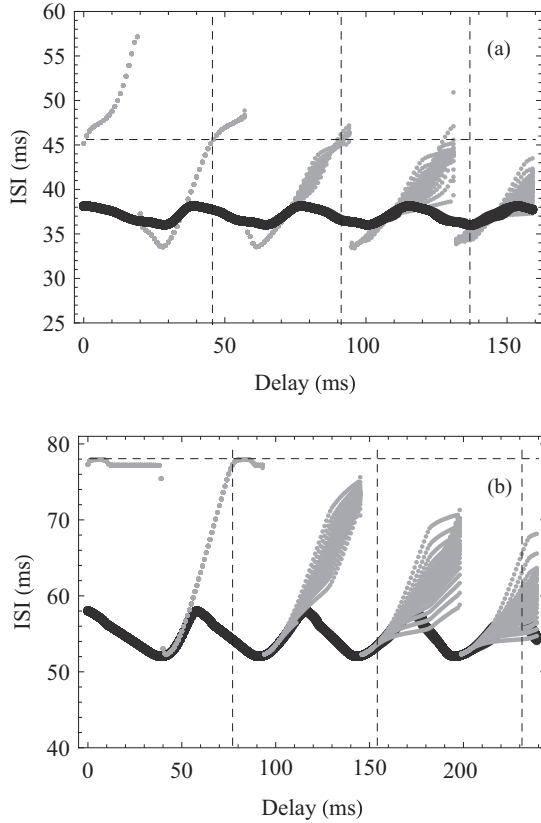


FIG. 6. Interspike intervals of a FN oscillator vs loop delay time with a feedback via a fast (gray points) and slow (black thick line) chemical excitatory synapse. In (a) and (b) the oscillators have been chosen from type II and type I, as described by the Eqs. (2.5) and (2.6), respectively. In both plots  $v_{th} = -0.5$ ,  $E_{syn} = +1.2$  (excitatory synapse) and  $g_{syn} = 0.1$ . External current is  $I_{ext} = 0.35$  in (a) and  $I_{ext} = 0.8$  in (b). The horizontal dashed lines show the intrinsic period of firing (without feedback) and the vertical dashed lines show the multiples of intrinsic period of firing.

action potential and the feedback induced input may not suffice to activate the neuron. We note here, for the HH model with subthreshold oscillations, when there is no repetitive firing, the period of these oscillations determines the intrinsic time scale which with the feedback induced time constant determines the behavior of the system. ISI plots in Fig. 7 show that although the period of subthreshold oscillations influences the dynamics of the neuron, the ISI is solely determined by the loop time delay once the neuron is in the repetitive spiking state.

IV. TWO NEURON LOOPS

Van der Sande *et al.* showed that when the elements in the loop evolve chaotically, with increasing the number of oscillators in the ring configuration, the spectral properties of the individual elements lose the fingerprint of the round trip time [3]. Here we show that basic properties of the one element loop discussed above is maintained in chains with more neurons. In the simplest case, two neurons communicating bidirectionally, as in Fig. 1(b), form a chain appearing in many canonical circuits in neural systems [26].

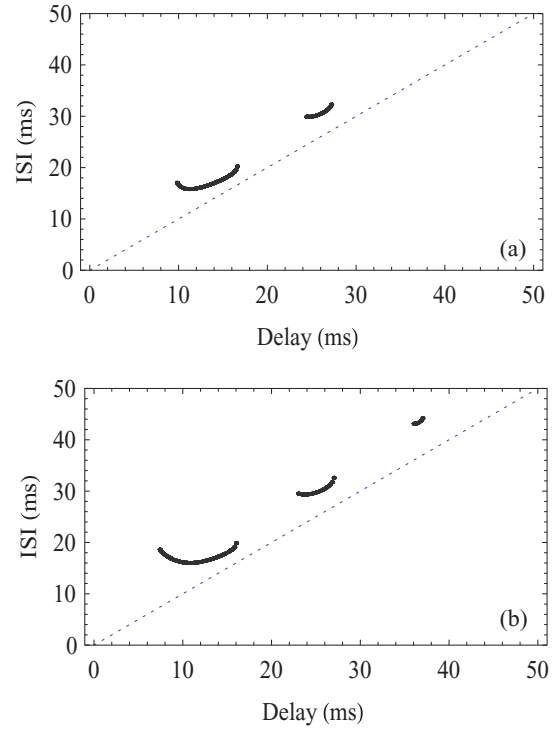


FIG. 7. (Color online) Interspike intervals of the neuron when it is biased by a subthreshold step current  $I_{ext} = 5$  for a fast (a) and slow (b) excitatory chemical synapse with the strength  $g_{syn} = 0.05$ . The dotted lines again show the relation of ISI with the loop delay time.

Each of the two synapses present in the model can be chosen to be fast or slow. When the communication in both paths is done with similar, fast or slow excitatory synapses, it is reasonable to expect the behavior of the system to be the same as the one neuron loop with a fast or a slow synapse, respectively. Our numeric results confirm this expectation. The nontrivial result arises when the synapses are chosen from different types: a fast and a slow synapse. Figure 8 shows the results when all the parameters of the neurons are the same and the round trip time is divided equally between the two paths.

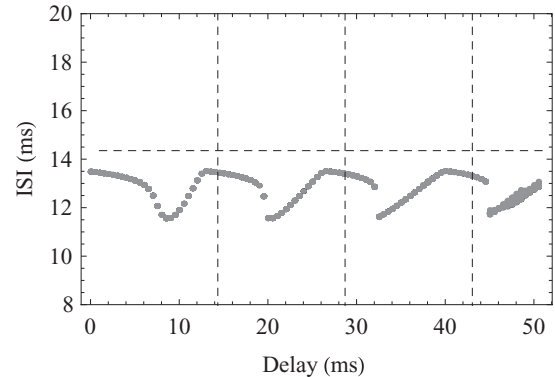


FIG. 8. Interspike intervals of two neurons interacting bidirectionally in a loop via two chemical excitatory synapses of different types: one fast and one slow. The horizontal axis shows round trip time, which is divided equally between two paths. All the parameters of the neurons and synapses are the same as in Fig. 2.

Surprisingly the results are quite similar to those of the single neuron loop with the slow synapse and the firing rate of both neurons is always more than their intrinsic firing rates. We have repeated the numeric tests with more than two elements (e.g., four neurons) and it is seen that existence of one slow synapse in the loop is enough to wash out the signature of the fast synapses (discussed in Sec. III) and the whole system shows the behavior which is expected from the single element loop with a slow synapse.

From arguments in the previous section it can be deduced that an input pulse, if lasts in time scales comparable with the intrinsic period of the neuron, advances the next spike each time they are imposed, regardless of where on the limit cycle they begin to act. So in the two neuron system we considered above, the one with slow afferent synapse tends to produce spikes with a larger rate and acts as the faster element in the loop. This fast oscillator goes on to determine the behavior of the whole system when the number of the oscillators in the loop increases. One should note here that each element of the system is determined by the neuron itself plus its incoming synapse, and with our choice of the same parameters for all the neurons; the difference in the incoming synapse determines which neuron is faster and has a leading role in the chain. Such particular role of the fast elements in the system of coupled oscillators has been reported for coupled integrate-fire systems [39], in the chains of coupled Josephson junctions [40], and also in brain research [41].

## V. DELAY INDUCED RESONANT STEPS

If the open loop neuron is in the resting state, due to the initial conditions, a strong enough feedback loop may excite the neuron to fire repeatedly. In this case the feedback delay determines solely the time constant of the activity of the system as it is seen in Fig. 7. If we fix the delay time constant, this fact will result in plateaus in the firing rate-input current characteristic of the neuron, which can be called *delay induced resonant steps*. In Fig. 9 we have shown such a characteristic for the system with the electrical synapse and also with fast and slow chemical synapses. It can be seen that all types of the synapses may cause delay induced steps on the characteristic firing rate determined by the delay time  $f_d = 1/\tau$ . Higher order steps on the multiple of the  $f_d$  can also occur but they are smoothed and eventually disappear for the system with slow synapses.

The appearance of the first step depends on the initial condition; existence of a single action potential in the interval  $[-\tau, 0]$  leads to the first step but the other steps can be seen even if the neuron is in the rest state during the initial period. In general, the order of the resonant steps is determined by the number of the effective feedback pulses (those which result in an action potential) in every time window equal to  $\tau$ : on the second step, before the feedback pulse arrives in neuron, the neuron fires another action potential, which leads to the doublets for each feedback period. Here despite what is shown in Fig. 3(b), both the feedback pulses of doublets lead to action potentials, resulting in a firing rate equal to  $2f_d$  and so on for other existing steps. We just mention that such steps are not seen in the characteristic of the system with inhibitory

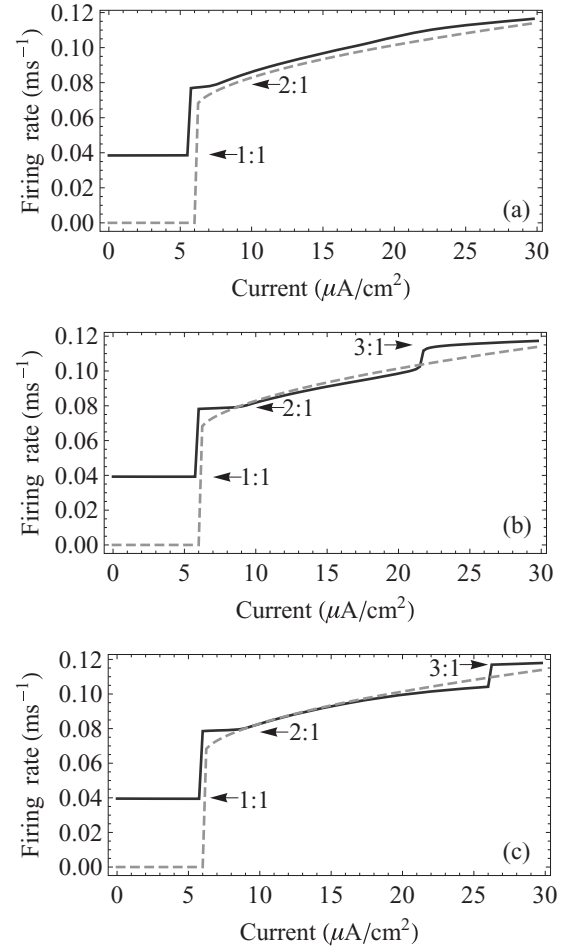


FIG. 9. Characteristics of the system, average firing rate of the neuron vs input current is plotted for the open loop neuron (dashed) and in presence of delayed feedback with (a) slow and (b) fast excitatory synapses, and (c) with an electrical synapse. The time delay is set by  $\tau = 25$  ms and the synaptic strength  $g_{el} = g_{syn} = 0.05$ .

synapses; it is again worth noting that in such systems, the loop time constant is not revealed when the feedback is inhibitory.

These steps are generic for all neuronal models, e.g., they can be seen in the characteristic of a simple leaky integrate-and-fire (LIF) neuron. For the simple model studied here, the pulses produced by the neuron circulate in the loop and act as a periodic input on the neuron itself where they can entrain the dynamics of the neuron. Considering the effect of the delayed feedback loop as an external periodic force brings the notion of *external synchronization* [42] in which a nonlinear oscillator is entrained by the external force. Such a phenomenon is well known for the Josephson junctions as the Shapiro steps [43] and also in the loops of coupled Josephson junctions, where the excitations move along the loop as solitary waves, and serve as an extra periodic force on the components of the system [44].

## VI. CONCLUSION

Delayed feedback loops introduce a new time scale into the dynamics of the system, determined by the circulation time. In the neural systems with chemical synapses, the connections remain active in the time scales, which may be comparable

with the intrinsic time scales of the neurons and the delay induced time scale. This opens the question of how the activity time of the synapses influences the behavior of the coupled neurons. In this work we addressed this question for the HH neurons coupled in a chain. The results have been shown to be applicable to the chains of the coupled relaxation oscillators, which inherit the basic phase space properties of the HH equations.

Defining fast and slow synapses in reference with the intrinsic time constants of the neuron, for a single neuron loop it was shown that different qualitative behaviors may arise in the feedback system. Gómez *et al.* showed that with a small strength self-excitation feedback both increase and decrease of the firing rate is possible [25]. Here we showed that this observation also depends on the duration of synaptic activity and besides strong self-excitation, long duration of the synaptic activity may also cover the fine structure properties of the model phase space, i.e., feedback via a slow excitatory synapse always speeds up the firing. On the other hand, decrease of firing rate of the neuron can be seen when strength of self-coupling is small and the activity time of the synapse is short (compared to the period of the firing). This behavior is related to the type of excitability of the HH model, which leads to phase-reset curves with large negative regions.

We also investigated how the interspike intervals are influenced by feedback. Again the nontrivial effects are seen for the fast synapses: due to the circulation delay time, the ISI of the open loop neuron may remain intact or change in the presence of feedback; but an interesting phenomenon may occur in which both the time scales of the open loop neuron and the feedback delay appear in the dynamics of the neuron. In this regime two subsystems of the neuron and the feedback loop behave as noninteracting and both time scales survive in the dynamics of the system. These phenomena are seen when the delay time exceeds the period of the open loop neuron, which has not been considered in [25], and are washed out again when the synaptic activity time is long.

In a more realistic model for the loops consisting of more than a single neuron, our results show that when all the synapses are from a single type, fast or slow but not both, the behavior of the system would be similar to that of a one neuron loop as is expected. With dissimilar synapses, e.g., when at least one of the synapses is slow, the dependence of the firing rate on the delay time is similar to that of the loop with a single neuron having a slow synapse. In a loop consisting of several firing neurons, the faster wins to control the behavior of the system. Here the neuron with slow afferent synapse, would fire faster and would lead the dynamics of the other neurons in the loop.

With the loops with inhibitory synapses, the results do not show any strict dependence of the behavior of the system on the activity time of the synapse, and the feedback loop via inhibitory synapses always slows down the rate of the firing. Also the system cannot be entrained by the inhibitory pulses in the loop, despite the excitatory pulses, which can synchronize the firing of the neuron.

It is well known that an external periodic force can entrain the dynamics of the nonlinear oscillators such that the frequency of the forced oscillator is determined by an integer (or rational) multiple of the external frequency [42]. In systems

with internal competing time scales, similar phenomena can occur, known as *self-induced resonance*, when the two time scales are of the same order [45]. Here we reported similar phenomena in which the external periodic force is replaced by the circulating excitation through feedback loop. Considering firing rate and external current as the output and input, respectively, in the characteristic diagram of the system, which shows the input-output relation, such a resonance appears as the plateaus in multiples of the inverse of the delay time.

## ACKNOWLEDGMENTS

Authors gratefully acknowledge an unknown referee whose remarks considerably improved the paper. A.V. acknowledges

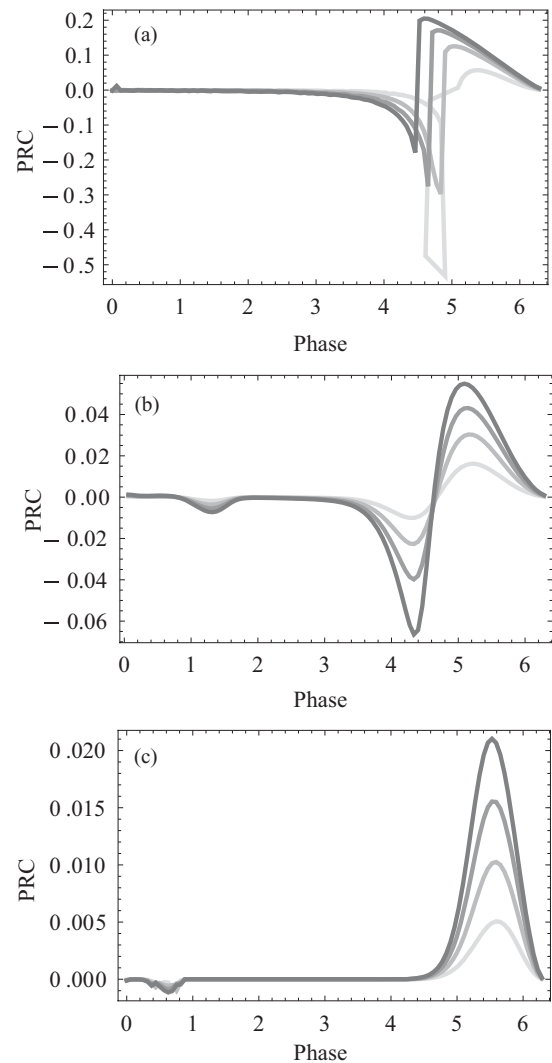


FIG. 10. Phase reset curves for the (a) HH model Eqs. (2.1) and (2.2), and (b) the type-II and (c) type-I models introduced by Eqs. (2.5) and (2.6), respectively. Horizontal axis shows the phase in which a pulse of duration 1 ms is imposed on the model neuron. Results are given for four different values of pulse amplitude: in (a), from light to dark gray the amplitude of the pulse is varied from 1 to 4 by increments 1. In (b) and (c), from light to dark gray, the amplitude of the pulse is varied from 0.01 to 0.04 by increments 0.01.



support by the Institute for Advanced Studies in Basic Sciences (IASBS) Research Council under Grant No. G2009IASBS109.

#### APPENDIX: PHASE RESET CURVES

For a periodically spiking neuron with period  $T$ , we define a uniformly increasing phase  $\phi$  as

$$\phi = \frac{2\pi}{T}(t - t_i), \quad (\text{A1})$$

where  $t_i$  is the time of the last spike [29]. Imposing a pulse of duration 1 ms in different phases on the limit cycle after the  $i$ th spike, the timing of the next spike  $t_{i+1}$  is recorded and the phase reset  $\Delta$  is defined as [18]

$$\Delta = 1 - \frac{t_{i+1} - t_i}{T}. \quad (\text{A2})$$

In Fig. 10, phase reset curves for the three models described in Sec. II are shown.

- 
- [1] R. Milo, S. Shen-Orr, S. Itzkovitz, N. Kashtan, D. Chklovskii, and U. Alon, *Science* **298**, 824 (2002); T. Nowotny and M. I. Rabinovich, *Phys. Rev. Lett.* **98**, 128106 (2007); S. Itzkovitz and U. Alon, *Phys. Rev. E* **71**, 026117 (2005); N. Kashtan, S. Itzkovitz, R. Milo, and U. Alon, *ibid.* **70**, 031909 (2004).
- [2] O. D’Huys, R. Vicente, T. Erneux, J. Danckaert, and I. Fischer, *Chaos* **18**, 037116 (2008).
- [3] G. Van der Sande, M. C. Soriano, I. Fischer, and C. R. Mirasso, *Phys. Rev. E* **77**, 055202(R) (2008).
- [4] D. Debanne, B. H. Gahwiler, and M. Thompson, *J. Physiol. (London)* **507**, 237 (1998).
- [5] A. Bacci, J. R. Huguenard, and D. A. Prince, *J. Neurosci.* **23**, 859 (2003); *Neuron* **49**, 119 (2006).
- [6] D. Debanne, B. H. Gahwiler, and S. M. Thompson, *J. Physiol.* **507**, 237 (1998); K. Nakazawa, M. C. Quirk, R. A. Chitwood, M. Watanabe, M. F. Yeckel, L. D. Sun, A. Kato, C. A. Carr, D. Johnston, M. A. Wilson, and S. Tonegawa, *Science* **297**, 211 (2002).
- [7] N. MacDonald, *Biological Delay Systems: Linear Stability Theory* (Cambridge University Press, Cambridge, England, 1989).
- [8] G. M. Suel, J. García-Ojalvo, L. M. Liberman, and M. B. Elowitz, *Nature (London)* **440**, 545 (2006).
- [9] K. Mergenthaler and R. Engbert, *Phys. Rev. Lett.* **98**, 138104 (2007).
- [10] J. L. Cabrera and J. G. Milton, *Phys. Rev. Lett.* **89**, 158702 (2002).
- [11] S. Bauer, O. Brox, J. Kreissl, B. Sartorius, M. Radziunas, J. Sieber, H.-J. Wünsche, and F. Henneberger, *Phys. Rev. E* **69**, 016206 (2004); W. S. Lam, P. N. Guzdar, and R. Roy, *ibid.* **67**, 025604(R) (2003); J. M. Mendez, R. Laje, M. Giudici, J. Aliaga, and G. B. Mindlin, *ibid.* **63**, 066218 (2001); M. Giudici, C. Green, G. Giacomelli, U. Nespolo, and J. R. Tredicce, *ibid.* **55**, 6414 (1997).
- [12] K. Konishi, *Phys. Rev. E* **70**, 066201 (2004); X. L. Deng and H. B. Huang, *ibid.* **65**, 055202(R) (2002); H. J. Wang, H. B. Huang, and G. X. Qi, *ibid.* **71**, 015202(R) (2005); M. Y. Kim, R. Roy, J. L. Aron, T. W. Carr, and I. B. Schwartz, *Phys. Rev. Lett.* **94**, 088101 (2005).
- [13] W. Gerstner and J. L. van Hemmen, *Phys. Rev. Lett.* **71**, 312 (1993); P. C. Bressloff, S. Coombes, and B. de Souza, *ibid.* **79**, 2791 (1997); P. C. Bressloff and S. Coombes, *ibid.* **80**, 4815 (1998); S. Kim, S. H. Park, and C. S. Ryu, *ibid.* **79**, 2911 (1997).
- [14] Y. Nakamura, F. Tominaga, and T. Munakata, *Phys. Rev. E* **49**, 4849 (1994); C. van Vreeswijk, *ibid.* **54**, 5522 (1996); U. Ernst, K. Pawelzik, and T. Geisel, *ibid.* **57**, 2150 (1998); E. M. Izhikevich, *ibid.* **58**, 905 (1998).
- [15] Y. Xia, M. Fu, and P. Shi, *Analysis and Synthesis of Dynamical Systems with Time-Delays* (Springer-Verlag, Berlin, Heidelberg, 2009).
- [16] J. Foss, A. Longtin, B. Mensour, and J. Milton, *Phys. Rev. Lett.* **76**, 708 (1996); J. Foss, F. Moss, and J. Milton, *Phys. Rev. E* **55**, 4536 (1997).
- [17] S. Yanchuk and P. Perlikowski, *Phys. Rev. E* **79**, 046221 (2009); M. S. Baptista and I. L. Caldas, *ibid.* **58**, 4413 (1998).
- [18] J. Foss and J. Milton, *J. Neurophysiol.* **84**, 975 (2000).
- [19] J. Simonet, E. Brun, and R. Badii, *Phys. Rev. E* **52**, 2294 (1995).
- [20] G. Kociuba and N. R. Heckenberg, *Phys. Rev. E* **68**, 066212 (2003); A. Ahlborn and U. Parlitz, *Phys. Rev. Lett.* **93**, 264101 (2004); A. G. Balanov, N. B. Janson, and E. Schöll, *Phys. Rev. E* **71**, 016222 (2005).
- [21] R. Femat and G. Solis-Perales, *Robust Synchronization of Chaotic Systems via Feedback* (Springer-Verlag, Berlin, 2008).
- [22] M. G. Rosenblum and A. S. Pikovsky, *Phys. Rev. Lett.* **92**, 114102 (2004); D. Goldobin, M. G. Rosenblum, and A. Pikovsky, *Phys. Rev. E* **67**, 061119 (2003).
- [23] O. Diez-Martinez and J. P. Segundo, *Biol. Cybern.* **47**, 33 (1983).
- [24] K. Pakdaman, J. F. Vibert, E. Boussard, and N. Azmy, *Neural Networks* **9**, 797 (1996).
- [25] L. Gómez, R. Budelli, and K. Pakdaman, *Phys. Rev. E* **64**, 061910 (2001).
- [26] I. Fischer, R. Vicente, J. M. Buldú, M. Peil, C. R. Mirasso, M. C. Torrent, and J. García-Ojalvo, *Phys. Rev. Lett.* **97**, 123902 (2006); R. Vicente, L. L. Gollo, C. R. Mirasso, I. Fischer, and G. Pipa, *Proc. Natl. Acad. Sci.* **105**, 17157 (2008); G. B. Ermentrout and N. Kopell, *ibid.* **95**, 1259 (1997).
- [27] C. Masoller, M. C. Torrent, and J. García-Ojalvo, in *Proceedings of the International Conference on Artificial Neural Networks*, edited by J. Marques de Sá, L. A. Alexandre, W. Duch, and D. P. Mandic (Springer-Verlag, Berlin, Heidelberg, 2007), pp. 963–972; C. Masoller, M. C. Torrent, and J. García-Ojalvo, *Phys. Rev. E* **78**, 041907 (2008); M. Sainz-Trapága, C. Masoller, H. A. Braun, and M. T. Huber, *ibid.* **70**, 031904 (2004).
- [28] B. Ermentrout, *Neural Comput.* **8**, 979 (1996).
- [29] E. M. Izhikevich, *Dynamical Systems in Neuroscience* (MIT, Cambridge, MA, 2007).
- [30] W. Gerstner and W. M. Kistler, *Spiking Neuron Models* (Cambridge University Press, Cambridge, England, 2002); P. Dayan and L. F. Abbott, *Theoretical Neuroscience* (MIT, Cambridge, MA, 2001).

- [31] S. G. Lee, A. Neiman, and S. Kim, *Phys. Rev. E* **57**, 3292 (1998); D. Hansel, G. Mato, and C. Meunier, *ibid.* **48**, 3470 (1993); H. Fukai, S. Doi, T. Nomura, and S. Sato, *Biol. Cybern.* **82**, 215 (2000).
- [32] A. L. Hodgkin and A. F. Huxley, *J. Physiol. (London)* **117**, 500 (1952).
- [33] We note that despite the chemical synapses, gap junctions have no threshold for activation. But since the signals in the delayed loop are assumed to be transmitted by axons and sub-threshold oscillations cannot be transmitted by axons, the threshold function is also considered in modeling the gap junctions.
- [34] R. Fitzhugh, *Biophys. J.* **1**, 445 (1961); J. S. Nagumo, S. Arimoto, and S. Yushizawa, *Proc. IRE* **50**, 2061 (1962); C. Rocșoreanu, A. Georgescu, and N. Giurgiteanu, *The Fitzhugh-Nagumo Model* (Kluwer Academic, Dordrecht, 2000).
- [35] With  $v = -1$ , which shows the minimum of the  $v$  nullcline,  $w$  nullcline for the large  $\eta$  can be approximated by the horizontal line  $w = 0$ . The cubic  $v$  nullcline and horizontal  $w$  nullcline (near the bifurcation point) prepare a canonical form of type-I excitability and undergo a saddle-node bifurcation in  $v = -1$  and  $w = 0$  when  $I_{\text{ext}} = 2/3$ ; see Ref. [36].
- [36] N. Berglund and B. Gentz, in *Stochastic Methods in Neuroscience*, edited by C. Laing and G. J. Lord (Oxford University Press, New York, 2010), pp. 65–93.
- [37] ISI plots show the intervals between each two successive spikes. So, finite points for a value of parameter (delay time) show that the behavior of the system is periodic and in this case the number of points indicates the number of intervals in a single period of the system. In the case of a chaotic behavior the points fill a subset of all possible values for large integration time. In this regard these plots are similar to a *Poincaré map* of a dynamical system and can be considered as a bifurcation diagram showing transition between periodic and aperiodic states.
- [38] E. Schöl, G. Hiller, Ph. Hövel, and M. A. Dahlem, *Philos. Trans. R. Soc. London, Ser. A* **367**, 1079 (2009).
- [39] A. N. Burkitt, *Biol. Cybern.* **95**, 97 (2006).
- [40] A. Valizadeh, M. R. Kolahchi, and J. P. Straley, *Phys. Rev. B* **82**, 144520 (2010).
- [41] C. T. Li, M. Poo, and Y. Dan, *Science* **324**, 643 (2009).
- [42] A. Pikovsky, M. Rosenblum, and J. Kurths, *Synchronization: A Universal Concept in Nonlinear Sciences* (Cambridge University Press, Cambridge, England, 2003).
- [43] S. Shapiro, *Phys. Rev. Lett.* **11**, 80 (1963).
- [44] H. S. J. van der Zant, T. P. Orlando, S. Watanabe, and S. H. Strogatz, *Phys. Rev. Lett.* **74**, 174 (1995); S. Ryu, W. Yu, and D. Stroud, *Phys. Rev. E* **53**, 2190 (1996).
- [45] A. Larsen, H. D. Jensen, and J. Mygind, *Phys. Rev. B* **43**, 10179 (1991); P. Barbara, A. B. Cawthorne, S. V. Shitov, and C. J. Lobb, *Phys. Rev. Lett.* **82**, 1963 (1999); M. A. Sarkisyan, *Sov. J. Quantum Electron.* **19**, 153 (1989).